THE ASTROPHYSICAL JOURNAL, 401:529–542, 1992 December 20

HUBBLE SPACE TELESCOPE FAINT OBJECT SPECTROGRAPH AND GROUND-BASED OBSERVATIONS OF THE BROAD ABSORPTION LINE QUASAR 0226−1024[1,2,3]

KIRK T. KORISTA, RAY J. WEYMANN, AND SIMON L. MORRIS
Observatories of the Carnegie Institution of Washington, 813 Santa Barbara Street, Pasadena, CA 91101
MICHAEL KOPKO, JR., AND DAVID A. TURNSHEK
University of Pittsburgh, Department of Physics and Astronomy, 100 Allen Hall, Pittsburgh, PA 15260
GEORGE F. HARTIG
Space Telescope Science Institute, 3700 San Martin Drive, Baltimore, MD 21218
CRAIG B. FOLTZ
Multiple Mirror Telescope Observatory, University of Arizona, Tucson, AZ 85721
AND
E. MARGARET BURBIDGE AND VESA T. JUNKKARINEN
Center for Astrophysics and Space Sciences, UC San Diego, 9500 Gilman Drive, La Jolla, CA 92093
Received 1992 March 30; accepted 1992 June 8

ABSTRACT

Faint Object Spectrograph data from the *Hubble Space Telescope* of the broad absorption line quasar 0226−1024 have revealed the presence of 8–10 absorbing ions between 680 and 1000 Å (restframe): C III, N III, N IV, O III, O IV, O VI, S V, S VI, possibly Ne VIII, and possibly O V* arising from a metastable excited state. We also present ground-based optical observations of the broad absorption line troughs for the following ions: H I, C IV, N V, Si IV, and possibly Fe III, S IV, P V, and C III* (also arising from a metastable excited state). The absorption line spectrum is fitted remarkably well using the observed C IV optical depth versus velocity as a template with arbitrary scale factors for the other ions. The results of this fit are used to estimate the absorbing ionic column densities. If broad absorption due to the excited state transition of O V λ760 is present, it implies very high electron densities and temperatures in the absorbing gas. There is evidence that the broad absorption line clouds are optically thick and either do not completely cover the continuum source or narrow unresolved lines are present.

Subject headings: line: identification — quasars: absorption lines — quasars: individual (0226−1024)

1. INTRODUCTION

Roughly 10% of all optically selected quasars exhibit broad, blueshifted absorption troughs which can extend to outflow velocities of 0.1–0.2*c*. These troughs are generally observed in C IV λ1549, Si IV λ1397, N V λ1240, and Lyα λ1216. A minority (perhaps ∼10%–20%) of these broad absorption line quasars (BALQSOs) exhibit broad absorption due to the lower ionization species of Mg II λ2798 and/or Al III λ1857, in addition to the other ions of higher ionization.

There are three primary questions about BALQSOs which investigators have attempted to answer.

1. Do BALQSOs and radio-quiet non–BALQSOs belong to the same population? If they do, then all QSOs have BAL clouds with a small covering factor roughly equal to the fraction of all QSOs which show BAL troughs (but see Morris 1988), and one observes a QSO as a BALQSO only at an appropriate orientation. The BALQSOs and non–BALQSOs should also have similar observational properties, other than the BALs. If BALQSOs are a different population of quasars, then the BAL clouds must have a covering factor of nearly unity in these objects, and one would not necessarily expect the two populations to have similar observational properties. Several studies have summarized the spectroscopic properties of BALQSOs and compared them to a sample of optically selected "normal" QSOs without broad absorption lines; these include Turnshek (1984a), Hartig & Baldwin (1986), Junkkarinen, Burbidge, & Smith (1987), and most recently Weymann et al. (1991) and Stocke et al. (1992).

2. What is the origin, the geometric distribution and covering factor, and the dynamical nature of the BAL clouds? Studies here include Junkkarinen (1983), Drew & Boksenberg (1984), Weymann, Turnshek, & Christiansen (1985), Surdej & Hutsemekers (1987), Turnshek (1988), Braun & Milgrom (1990), Begelman, de Kool, & Sikora (1991), and Hamann, Korista, & Morris (1992).

3. What are the physical properties (e.g., ionization, temperature, chemical abundances) of the BAL clouds? Several investigators have delved into this question through studies of the estimated ionic column densities and/or temporal variations of the BAL troughs (Turnshek 1984b; Turnshek et al. 1984; Junkkarinen et al. 1987; Turnshek et al. 1987; Smith & Penston 1988; Junkkarinen, & Burbidge 1989; Kwan 1990; Barlow et al. 1992).

There are no clear answers yet to any of these questions. However, all previous studies have been limited to the study of a few of the ions mentioned above: C IV, Si IV, N V, Lyα, and occasionally O VI and C III. In this paper we present combined

[1] Some of the observations reported here were made with the NASA/ESA/*HST*, obtained at the STScI, which is operated by AURA, Inc., under NASA contract NAS5-26555.

[2] Some of the observations reported here were made with the Multiple Mirror Telescope, a facility operated jointly by the University of Arizona and the Smithsonian Institution.

[3] Some of the observations reported here were made at Palomar Observatory as part of a collaborative agreement between the California Institute of Technology and the Carnegie Institution of Washington.

ground-based and *Hubble Space Telescope* (*HST*)–Faint Object Spectrograph (FOS) observations of the BALQSO 0226−1024, for which we find BAL troughs belonging to 12–18 separate ions. While some of these ions can, in principle, be studied from the ground from high-redshift BALQSOs, the much denser Lyα forest and the frequent occurrence of Lyman limit systems make this very difficult. In § 2 we present the FOS and optical observations and in § 3 we estimate the ionic column densities. We present a discussion of the results in § 4, and § 5 summarizes the results.

2. THE OBSERVATIONS

2.1. *The FOS Data*

The *HST* data were acquired on 1991 June 13 with the FOS red detector, with the G270H grating, after autonomous ("Binary Search") target acquisition into the 1″ circular aperture. Two 1000 s exposures were obtained, on consecutive orbits, in the standard ACCUM mode. Data reduction was performed at the STScI using IDL software developed by the FOS instrument team. The image drift induced by the geomagnetic field was removed using a model to compute the offset for each of the 125 s intervals between data readouts, then shifting the spectrum accumulated during each interval by integral quarter-diode steps to compensate, before co-adding. The background count rates were estimated by averaging many hours of dark calibration observations. The observed wavelength scale was determined from a previous onboard line source observation, which was also corrected for the geomagnetically induced image drift. No radial velocity correction was applied, and the wavelengths are in vacuo. Fixed pattern noise was removed using an observation of the white dwarf standard G191B2B, selected for its relatively featureless spectrum. Count rates were converted to fluxes using the mean inverse sensitivity curve developed from observations of three standard stars (BD +2804211, BD +3302642 and HZ 44). We estimate the error in the absolute flux calibration at ±15%, over the range of the spectrum, while the wavelength scale is accurate to approximately ±1.5 Å. The FWHM resolution is approximately 255 km s^{-1}. The FOS spectrum, together with the 1 σ error spectrum, is shown in Figure 1.

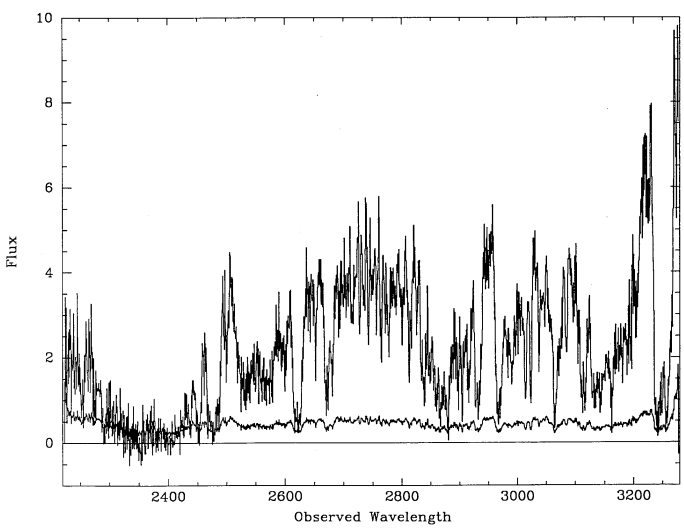

FIG. 1.—The G270H–FOS spectrum of 0226−1024. The formal 1 σ error spectrum is also shown. The observed flux is in units of 10^{-16} ergs s^{-1} cm^{-2} Å^{-1}.

2.2. *The Ground-based Optical Data*

Some of the optical data were obtained in 1987 September and 1989 October with the Multiple Mirror Telescope blue and red channel spectrographs, respectively. The effective wavelength coverage is 3270–9930 Å which for the adopted emission line redshift of 2.256 corresponds to roughly 1000–3050 Å in the rest frame of 0226−1024. The spectral resolution is roughly 120 km s^{-1} blueward of 4440 Å and 300 km s^{-1} to the red of this (near the C IV trough). Weymann et al. (1991) discuss in more detail the observations and summarize the emission and absorption line properties of this BALQSO.

Because the FOS data are so heavily absorbed by the BALs, it is difficult to determine the continuum level and shape. One would like to join the FOS data to the optical data to aid in the estimation of the continuum level and shape in the FOS data. However, there are only ∼20 Å overlap between the FOS and MMT data, and the MMT data are noisy in the overlap region so it was not possible to accurately join the optical MMT data to the FOS data. In addition, a small (2.″5 diameter) aperture was used in the MMT observation, thus the relative flux calibration is uncertain in the near-UV. Thus, in 1991 December, observations of 0226−1024 extending to ∼3120 Å were obtained with the Double Spectrograph of the Hale 5 m telescope. The spectral resolution was about 330 km s^{-1} in the blue (3120–4700 Å) and 660 km s^{-1} in the red (4700–9000 Å) for a 1″ slit. See Weymann et al. (1991) for a description of the data acquisition with this spectrograph. Care was taken to rotate the slit along the direction of atmospheric dispersion; wide-slit (4″ and 8″) observations were also obtained on a photometric night. There were no wavelength-dependent light losses in the narrow slit relative to the wide-slit Double Spectrograph observation.

Although we attempted to obtain absolute fluxes under photometric conditions, there is a disagreement between the derived ground-based flux from the 5 m observations and the FOS flux in the overlap region 3120–3270 Å; however, the shapes of the two spectra are quite similar. By multiplying the 5 m fluxes by 1.36, the two spectra agree quite well in the overlap region. Figure 2 shows the overlap region of the 4″. Double Spectrograph data with the FOS data after this scaling, and after smoothing the FOS data to match the resolution of the 5 m spectrum. Considering the quoted uncertainty in the FOS flux calibration, the uncertainty in the standard star fluxes used in the ground-based observations, the difficulty of determining accurate extinction in the extreme UV of the ground-based data and, finally, the fact that the FOS and 5 m observations were separated by about 6 months, the agreement in the relative fluxes is quite good and a disagreement of 36% in the absolute flux is not unreasonable.

Because the MMT observations are of higher resolution than the 5 m observations, we prefer them for the analysis of the C IV and S IV troughs. However, the relative fluxes in the near-UV are less reliable than the 5 m relative fluxes. Indeed, we found that the MMT data suffered from substantial wavelength-dependent loss of light starting blueward of roughly 4000 Å (near the rest frame Lyα emission). We therefore used the Double Spectrograph data blueward of 4200 Å (1290 Å rest frame). The final joint FOS and ground-based spectrum—which forms the basis for the rest of our analysis—is shown in Figure 3. The data have been shifted into the rest frame; the vertical axis has units of relative L_λ (ergs s^{-1} Å^{-1}), having been normalized to 1.0 near 2100 Å (see Weymann et al. 1991).

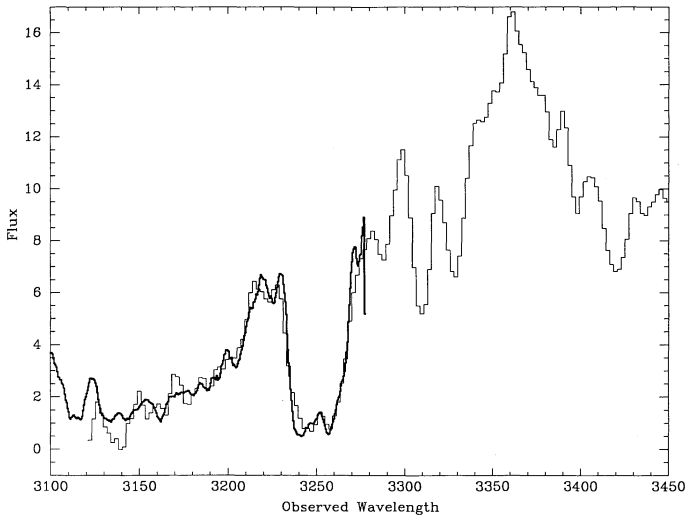

FIG. 2.—The FOS and the 4″ slit 5 m spectra in the region of overlap between the *HST* and ground-based data. The 5 m flux has been scaled by a factor of 1.36 to match the FOS flux, and the FOS spectrum has been smoothed to match the 5 m spectral resolution. Shown are the broad emission and broad absorption of O VI λ1034. The observed flux units are the same as in Fig. 1.

3. FITTING THE ABSORPTION LINE SPECTRUM AND DETERMINING THE IONIC COLUMN DENSITIES

3.1. *Candidate Absorption Line Troughs*

As described in detail in § 3.2 below, we devised an automatic algorithm to determine the ionic column densities of the various ions making significant contributions to the broad absorption in the FOS spectrum. The algorithm minimizes the difference between the observed FOS spectrum and a synthetic spectrum. As a first step in this process we drew up a list of all the ground-term multiplets which satisfied the following criteria:

Criterion 1:

$$\log [(f\lambda)_\lambda Ab(E)] - \log [(f\lambda)_{1548} Ab(C)] \gtrsim -2.0 , \quad (1)$$

where in the first term $f\lambda$ refers to the f-value and wavelength of the strongest transition in the multiplet in question, ignoring a factor of $g/\Sigma g$, and $Ab(E)$ is the relative number abundance of the element in question. The second term involves the corresponding quantities for the C IV λ1548 transition. Criterion (1) is equivalent to the statement that the optical depth of the strongest transition in the multiplet would be at least 1% of the C IV λ1548 optical depth if the fractional abundance of the ion in question were the same as the fraction of C which is C IV. Transitions which do not satisfy this criterion are almost certainly too weak to contribute significantly to the absorption unless there are very large abundance anomalies. In applying it, we used the compilation of wavelengths and f-values from Morton (1991, 1992); otherwise we used the data given in Wiese, Smith, & Glennun (1966), Wiese, Smith & Miles (1969). For the relative abundances we used the compilation of Grevesse & Anders (1989).

Criterion 2:

Transitions from neutral and singly ionized ions were ignored.

The justification for (2) arises from the fact that there is no indication of absorption troughs from λ1334 of C II in the ground-based data. Inspection of the ionization potentials of all other neutral and singly ionized ions with transitions satisfying (1) strongly suggests that none of them will contribute significant absorption either. The one possible exception to this is a multiplet of O II at λ834. Its ionization potential is slightly larger than the energy required to create Si IV (33.49 eV). Because the three transitions of O II are nearly coincident with three of the transitions in O III (the largest $\Delta\lambda = 0.8$ Å), we cannot establish its presence with any certainty. However, we expect O III to make the dominant contribution of the two oxygen ions, so that the O II ion was not included.

We also included the UV multiplet three excited state metastable transitions of O V λ760, N IV λ923, and C III λ1075, the first of these suggested by Pettini & Boksenberg (1986) to be in broad absorption in the BALQSO 0946+3009 based upon *IUE* data. Confirmation of a large column density in any of these transitions would be of great interest, as this would place a lower limit to the electron density in the BAL region and would imply high electron temperatures (see § 4.3).

The resulting list of candidate transitions is given in Table 1 and discussed in further detail below. We have assumed here that the relative abundances of the heavy elements are not vastly different from solar. It has been suggested that the heavy-element abundance in BAL clouds may be dramatically enhanced compared to solar values (e.g., Turnshek et al. 1987). If this is the case then there might also be significant departures from the solar values in the relative distribution of the heavy elements. In particular, Turnshek et al. (1987) suggest the presence of a trough arising from P V λ1121, which has creation and destruction ionization potentials very similar to C IV, in the BALQSO 1413+1143. If P V is present in 0226−1024 we would also expect a contribution from P IV λ951, whose creation and destruction ionization potentials are very similar to that of C III. We address this in § 3.3.

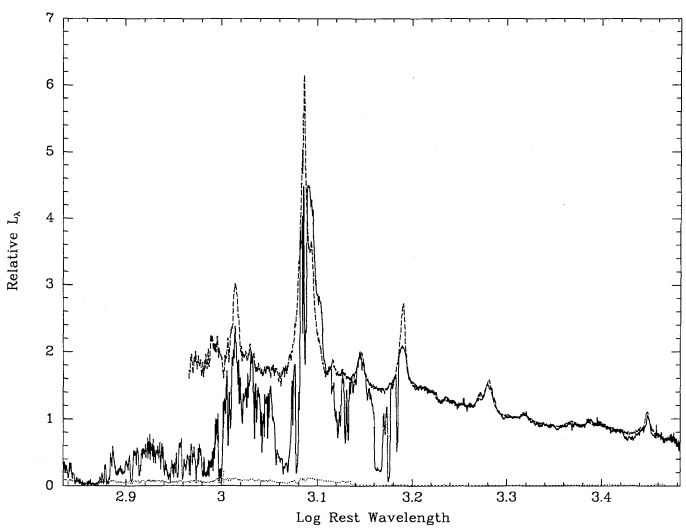

FIG. 3.—The combined FOS and ground-based spectrum of 0226−1024 (*solid*) with the accompanying 1 σ error spectrum (*dotted*). The FOS data have been smoothed to match the MMT red channel ground-based data spectral resolution. These are plotted on the same scale as the mean non–BALQSO spectrum from Weymann et al. (1991), shown with dashed lines. The ordinate has arbitrary units of ergs s^{-1} $Å^{-1}$. Note that a log λ scale has been used for the abscissa and that the wavelength scale is in the restframe of 0226−1024.

3.2. *Fitting the FOS Spectrum*

In regions of the spectrum where there is little or no overlap of the absorption troughs from different ions, estimating the column densities of each ion is relatively straightforward. However, the number of potential contributors to the absorption in the FOS region of the spectrum becomes sufficiently large that in order to fit the absorption line spectrum and derive the ionic column densities, we developed a more formal procedure as described in this section. We also apply this procedure to the ground-based data in § 3.3.

3.2.1. *Creating an Optical Depth Template*

The basic assumption underlying the fitting procedure is that the optical depth as a function of velocity for any transition is the same as that for the C IV absorption to within constant scale factors. We discuss the validity of this assumption in § 4.5. An optical depth template was created from the C IV absorption line profile, which is both strong and unblended with other absorption lines, as follows.

After normalizing the optical spectrum of 0226−1024 to 1.0 at 2100 Å, it bore a remarkable resemblance to the mean non–BALQSO spectrum of sample (1) from Weymann et al. (1991), selected from the Large Bright Quasar Survey (LBQS: see Foltz et al. 1987, 1989; Hewett et al. 1991; Chaffee et al. 1991; and Morris et al. 1991), also shown in Figure 3. Similarities are evident in emission-line strength and profile and in continuum shape redward of the Lyα–N V emission. There are, however, a few differences (see Fig. 3). In particular, the mean non–BALQSO emission line of C IV λ1549 is somewhat stronger than that of 0226−1024, though only deviating above the ∼60% intensity level of the emission line of the mean non–BALQSO line. Whether this difference is due to broad absorption or to intrinsic emission-line differences (or both) is unknown. In our analysis, any absorption lying within ∼3000 km s^{-1} of the emission-line peak was ignored in creating the template. We note here that the data blueward of roughly 1100 Å in the mean LBQS non–BALQSO spectrum consist of 10 radio-quiet LBQS QSOs, observed by three of us (K. T. K., R. J. W., and S. L. M.) since Weymann et al. (1991). The QSOs in this "extension" have a slightly larger mean redshift and luminosity than do those making up the remainder of the mean non–BALQSO spectrum. The mean non–BALQSO spectrum is plotted down to roughly 930 Å; blueward of this the spectrum rolls over due to intervening absorption, meeting the FOS flux near 850 Å.

The optical spectrum of 0226−1024 was then divided by the mean non–BALQSO spectrum, forming a residual intensity spectrum $I_r(\lambda)$. Assuming that (1) the BAL gas completely covers the continuum source for all outflow velocities, (2) the BAL contains no unresolved narrow lines, and (3) that any scattered light and emission from the BAL gas are negligible, then the optical depth τ is given by $\tau(\lambda) = -\ln [I_r(\lambda)]$. Note that we do not assume that the BAL troughs are optically thin, but note also that the failure of any of these assumptions to be valid acts to make the derived optical depth an underestimate of its true value. The observed residual intensity in the C IV trough is the result of absorption by both components of the C IV doublet, and the contribution of the weaker C IV doublet was then subtracted to form the final C IV optical depth template. The method of correcting for the presence of the doublet and its caveats is described in Junkkarinen, Burbidge, & Smith (1983). Figure 4 illustrates the final C IV λ1548 optical depth template.

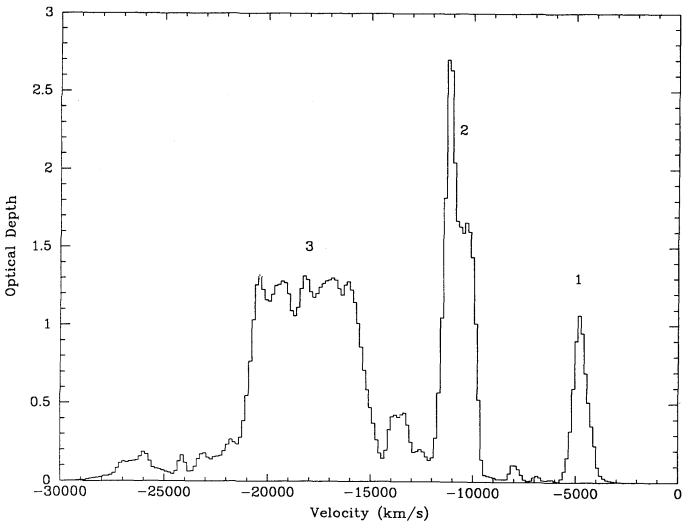

FIG. 4.—The adopted optical depth template, derived from the C IV λ1548 trough. The major troughs are labeled.

The C IV trough has three distinct major features (see Fig. 4): two narrow troughs at roughly −5000 km s^{-1} and −11,000 km s^{-1} and a third broad trough between roughly −15,000 km s^{-1} and −24,000 km s^{-1}, with respect to the systemic velocity defined by the broad emission lines (see Weymann et al. 1991). These will be referred to as troughs (1)–(3), respectively. Weaker features lie near −13,500 and −8000 km s^{-1}.

This template was then shifted into the rest wavelengths of each of the candidate transitions for the FOS absorption spectrum. If a ground-term multiplet consists of well-resolved components, then each component is represented by a shifted C IV optical depth template. In several instances, the ground-term multiplet is comprised of several transitions, some of which are not resolved at the FOS resolution. If two or more transitions within a multiplet were separated in velocity by significantly less than the spectral resolution, they were combined to form a single transition at a single mean wavelength with a single effective *f*-value. In computing this *f*-value the populations of the different levels in the ground terms were assumed to be proportional to their statistical weights.

Column (1) of Table 1 lists the elements considered along with the log of the abundances as given by Grevesse & Anders (1989). In columns (2)–(4) we give the list of ions considered and the ionization potentials required to create and destroy each ion. Column (5) gives the wavelengths and multiplet numbers of the candidate transitions considered (combined in some cases as indicated above) while column (6) gives the corresponding effective log ($gf\lambda$)-values. The last column lists the source for the wavelengths and *f*-values.

3.2.2. *The Continuum in the FOS Spectrum*

Because of the large amount of absorption present and unknown broad emission-line strengths, it was difficult to determine the continuum in the FOS data. We can state with some confidence that the continuum does not lie much above the observed data in the region between 825 and 860 Å, since this region should be clear of any strong broad absorption, although some contribution from O III emission in this region may be present. Lyα forest absorption and possible weak Lyman limit absorption systems are additional sources of uncertainty in the location of the continuum. We made no

TABLE 1

ATOMIC DATA

Element/logarithm[a] (1)	Ion (2)	IP (create) (eV) (3)	IP (destroy) (eV) (4)	λ/multiplet (5)	log (gfλ) (6)	Reference[b] (7)
Hydrogen 0.000	I	...	13.6	1215.7	3.005	1
Carbon −3.440	III	24.4	47.9	977.0 1 uv	2.872	1
				1175.7 4 uv	3.440	2
	IV	47.9	64.5	1548.2 1 uv	2.771	1
				1550.8	2.470	
Nitrogen −3.951	III	29.6	47.4	991.6 1 uv	2.625	1
				989.8	2.324	
				764.4 2 uv	2.377	3
				763.3	2.080	
	IV	47.4	77.5	765.1 1 uv	2.674	3
				923.2 3 uv	3.242	2
	V	77.5	97.9	1238.8 1 uv	2.590	1
				1242.8	2.289	
Oxygen −3.070	III	35.1	54.9	835.3 1 uv	2.645	3
				833.7	2.419	
				832.9	1.942	
				703.9 2 uv	2.667	3
				702.9	2.445	
				702.3	1.968	
	IV	54.9	77.4	790.2 1 uv	2.543	3
				787.7	2.242	
	V	77.4	113.9	760.4 3 uv	3.091	2
	VI	113.9	138.1	1031.9 1 uv	2.438	1
				1037.6	2.137	
Neon −3.910	VIII	207.3	239.1	770.4 1 uv	2.196	2
				780.3	1.894	
Silicon −4.450	IV	33.5	45.1	1393.8 1 uv	3.156	1
				1402.8	2.855	
Phosphorus −6.430	IV	30.2	51.4	950.7 1 uv	3.044	1
	V	51.4	65.0	1118.0 1 uv	3.024	1
				1128.0	2.723	
Sulfur −4.790	IV	34.8	47.3	1073.0 1 uv	2.231	1
				1062.7	1.929	
	V	47.3	72.7	786.5 1 uv	3.060	4
	VI	72.7	88.0	933.4 1 uv	2.916	1
				944.5	2.615	
Argon −4.440	V	59.8	75.0	835.0 1 uv	3.320	4
				827.1	3.102	
				822.2	2.623	
	VI	75.0	91.0	767.1 1 uv	3.175	4
				754.9	2.860	
	VIII	124.3	143.5	700.2 1 uv	2.726	4
				713.8	2.426	
Iron −4.330	III	16.2	30.7	1122.5 1 uv	2.901	1
				1124.9	2.612	
				1126.7	2.184	
				1128.1	2.663	
				1129.2	2.293	
				1130.4	1.940	
				1131.4	1.977	

[a] Element and logarithm of relative solar abundance by number.

[b] Source for wavelengths and *f*-values: (1) Morton 1991; (2) Wiese et al. 1966; (3) Morton 1992; (4) Wiese et al. 1969.

attempt to correct for the mean depression associated with Lyα blanketing, and since we do not possess a suitable non–BALQSO mean spectrum for this region of the spectrum, we have made no attempt to incorporate emission lines into the effective continuum for the BAL troughs (see § 3.3). This will also lead to an underestimate of the true optical depth. Because of all these uncertainties we have chosen to incorporate the continuum fitting as part of our algorithm for fitting the FOS absorption-line spectrum.

3.2.3. *The Fitting Algorithm for the FOS Spectrum*

The parameters defining the fit are the optical depth multipliers for all the candidate transitions of Table 1 and two parameters defining the continuum. The optical depth multiplier is the ratio of the optical depth of the transition to that of C IV λ1548. We fit the continuum with a power law given by an amplitude $F(\lambda_0)$ and the usual spectral index α ($F_\nu \sim \nu^\alpha$):

$$F_\lambda = F_{\lambda 0}(\lambda_0/\lambda)^{(2+\alpha)} \quad (2)$$

with λ_0 arbitrarily set at 1005 Å.

Only one optical depth multiplier associated with all the transitions from the ground term from each ion is a free parameter, since the optical depths for any other transitions involving the ground term of that ion are constrained by our assumption that the populations of the levels in the ground

term are distributed according to their statistical weights. (The metastable levels of C III, N IV, and O V are, effectively, separate ions). The free parameters are determined by minimizing χ^2 between the fit and observed spectra, using the FOS error spectrum as an estimate for the sigma.

Before carrying out this minimization, the FOS data were smoothed to the resolution of the MMT red channel data. To find a combination of the optical depth multipliers and the two parameters defining the continuum fit which gave a minimum in the χ^2 function (which is a highly nonlinear function of the free parameters), the "downhill simplex method" of AMOEBA (Press et al. 1986) was used. In general this meant there were 10–14 free optical depth multipliers and the two continuum fit parameters which were varied by AMOEBA, with 11–16 additional constrained optical depth multipliers (the number depending on how argon and Ne VIII were handled—see below). For readers interested in but unfamiliar with the downhill simplex method as implemented by AMOEBA we give a brief summary of its use in the following two paragraphs. Consult Press et al. (1986) for further details.

AMOEBA requires the specification of initial guesses for $(N + 1)$ N-dimensional vectors (where N is the number of free parameters in the minimization procedure). Each vector defines a vertex of an N-dimensional volume. The vertices are adjusted until the volume has shrunk so that the fractional difference between the largest and smallest values of the function being minimized (in our case χ^2) becomes less than some prescribed value (the convergence tolerance). The output from AMOEBA is thus a set of $(N + 1)$ different solutions each having a value of χ^2 very close to a true (possibly local!) minimum.

In a minimization procedure as complex as the present one, the final solutions may be dependent upon both the value of the fractional difference in χ^2 used in the convergence criterion, and, more importantly, upon the initial values of the free parameters input to AMOEBA, since there may be a large number of local minima in the multidimensional space being explored. In order to estimate the sensitivity of the resulting column densities and continuum fit to these initial conditions in a fairly objective way we followed the precept of Press et al.: We chose an initial continuum amplitude such that the input continuum was a factor of 2 higher than the highest point in the data, set the initial free optical multipliers to very small values (10^{-2}), and set the χ^2 tolerance to a very small value (10^{-7}). We then let AMOEBA reduce the continuum strength and increase the optical depth multipliers to find the deepest minimum. We then initiated a second pass with AMOEBA but with the initial guesses for the $(N + 1)$ starting vectors offset from the solution having the minimum χ^2 at the conclusion of the first pass. This iteration process was repeated usually twice more, or until the fluctuations in the column densities between two consecutive iterations became small (a few percent).

As discussed below, it proved impossible to determine whether or not there was any significant column density from Ne VIII, and since its possible presence is of special interest we ran three parallel series with AMOEBA in which the Ne VIII column density was first set to zero, then treated as a free parameter, and finally set to a minimum value which would account for the absorption feature near 768 Å. This absorption feature and its possible association with Ne VIII is discussed below.

By integrating the optical depth spectrum of C IV over velocity, we found a column density of $\log N(\text{C IV}) \geq 16.20$ cm^{-2}. We again stress that we do not assume that the transition is optically thin, but use the inequality sign to emphasize that all of the assumptions we have made act to underestimate the true optical depth, as noted above. Using this derived column density the other ionic column densities were determined from their optical depth multipliers and the atomic parameters of the particular transition (wavelength and f-value). Upon using the procedure described in the preceding paragraphs it became clear that the column densities of the ions of N IV and S V, as well as Ne VIII, are the most poorly determined. (An indication of this is found in the large differences in the column densities for these ions between the first and last passes of AMOEBA, exhibited in Table 2A, which is discussed below.) This is not surprising, since the troughs from these ions strongly overlap. Thus, the distinctive structure of the C IV optical depth template is blurred for these ions, and we cannot unambiguously determine their column densities. We note that despite the relatively small inferred column density of S V ($\sim 10^{15}$ cm^{-2}), its optical depth is significant (due to its large f-value), corresponding to roughly 20% the total optical depth in C IV. The results of the first pass of the first run indicated a large column in Ar VI ($> 10^{16}$ cm^{-2}). However, this possible significant overabundance of argon seems to be ruled out by the absence of a detectable Ar V trough which ought to have a strength comparable to or larger than that of Ar VI ($\geq 75\%$ the total optical depth of C IV). We estimate an upper limit in the column density of Ar V of about 6×10^{14} cm^{-2}, which corresponds to only 3% the total optical depth in C IV. We note that all of the major troughs of Ar V, except trough (1) of the λ827 transition located near 814 Å, fall within the major troughs of O III, and could be a source of confusion for the fitting (see Fig. 5*a*). However, other than the narrow, probably intervening, Lyα absorption just redward of the hypothetical position of trough (1) of the λ827 transition, there is no evidence for substantial absorption even after considering that the effective continuum in this region is high relative to the power law-fit because it probably lies on the blue wing of broad O III emission. We therefore considered a significant column density in Ar VI as unlikely and removed the argon ions from the subsequent fitting.

Table 2A contains the results for the runs described above with the column density for Ne VIII set to zero, as a free parameter, and with it set to a constant. Column (1) gives the names of the free parameters, column (2) gives the result of the first pass with AMOEBA while column (3) gives the result for the last pass, in both cases with Ne VIII set to zero. Columns (4) and (5) give the same information as columns (2) and (3) but for the case where the Ne VIII column density is a free parameter. Columns (6) and (7) give the same information as columns (2) and (3) but for the case where the Ne VIII column density is set to a constant. Column (8) is described below. Figures 5*a*, *b*, *c* illustrate the fits to the data using the column densities from columns (3), (5), and (7), respectively, from Table 2A.

Except for the ions affected by the possible Ne VIII absorption, the inferred optical depths are remarkably similar in all six runs listed in Table 2A. Thus we are confident that we indeed found the best fits to the FOS data, given our assumptions. Figure 6 illustrates the power-law continuum fit for the run shown in Figure 5*c*. The power-law continua predicted from the FOS fits are fairly consistent with any continuum that might be estimated by eye from the combined ground-based/FOS data. However, it is clear that the continuum we have determined in this way will not fit the continuum for the

TABLE 2A

FOS DATA

NAME (1)	No Ne VIII (2)	(3)	Ne VIII FREE (4)	(5)	Ne VIII CONSTANT (6)	(7)	KT (8)
Power-Law Fit Parameters							
$F_{\lambda 0}$	0.9342	0.9375	0.9870	0.9393	0.9715	0.9353	
$-\alpha$	5.209	5.263	5.607	5.276	5.595	5.246	
log (column density)							
C III	15.49	15.48	15.50	15.48	15.49	15.48	15.66
N III	16.30	16.30	16.32	16.30	16.32	16.30	16.27
N IV	16.37	16.82	16.00	16.74	15.71	16.70	16.28
N IV (excited)	15.13	15.06	15.05	15.05	15.06	15.08	...
O III	16.64	16.64	16.62	16.64	16.61	16.64	16.77
O IV	16.68	16.71	16.62	16.69	16.90	16.67	16.70
O V (excited)	16.40	16.29	16.69	16.39	16.23	16.40	...
O VI	16.51	16.51	16.53	16.51	16.52	16.51	16.38
Ne VIII	...	...	16.46	16.04	16.57	16.57	16.56
S V	15.17	15.14	15.11	15.05	12.17	14.82	...
S VI	15.94	15.94	15.95	15.94	15.93	15.94	15.92
Ar V	13.60						
Ar VI	16.14						16.25
Ar VIII	14.78						

TABLE 2B

GROUND-BASED DATA

Ion (1)	log (Column Density) (2)	log (Column Density): KT (3)
H I	15.90 (15.84)	15.76
C III (excited)	15.73	
C IV	16.20	16.18
N V	16.37 (16.31)	16.36
O VI	16.69 (16.44)	16.38
Si IV	15.32	15.12
S IV	16.56	
P V	15.29 ?	15.06
Fe III	15.74, 16.30	15.57

ground-based data longward of about Lyα and is not at all consistent with the mean non–BALQSO spectrum from Weymann et al. As noted in Weymann et al. some mechanism appears to depress the continuum in the BALQSOs relative to the non–BALQSOs in addition to the obvious broad absorption troughs themselves. This effect becomes more pronounced the bluer one goes, consistent with what we find in 0226−1024 (see Fig. 3). This effect is even more striking in the Mg II BALQSOs (Weymann et al. 1991; Sprayberry & Foltz 1992), and the latter authors present a plausible case for extinction by dust. A more sophisticated treatment of the continuum must await an understanding of this phenomenon.

3.3. *Fitting the Optical Spectrum*

Fitting the optical spectrum was done in much the same way as for the FOS data with the following important exception: Rather than characterize the continuum by two free parameters we adopted the mean non–BALQSO spectrum described above as the effective continuum. This has the advantage that it incorporates the emission lines into the effective continuum. Implicit in this are the assumptions that the BAL clouds lie completely outside both the true continuum-forming regions and the broad emission-line regions as well as that the emission-line strengths and profiles in the mean non–BALQSO spectrum do not differ markedly from those which would be seen in 0226−1024 in the absence of the absorption troughs. The fact that N V absorption extending to −6000 km s^{-1} invariably strongly attenuates Lyα emission supports the former assumption while the general result of Weymann et al. (1991) on the similarities between the BALQSO and non–BALQSO emission-line properties supports the latter.

As noted in § 3.2.1, however, there are differences in the C IV profile between the mean non–BALQSO spectrum and 0226−1024. In addition, as found to be true in a large sample of BALQSOs by Weymann et al. (1991), the region near the emission line center of N V λ1240 is enhanced in the spectrum of 0226−1024, relative to the mean non–BALQSO spectrum. The nature of the enhancement near N V is still unclear. As noted above however, the C IV template ignores any absorption within 3000 km s^{-1} of the broad emission lines so this region is ignored in deriving the N V column density.

An additional difference was described at the end of the last section. Blueward of the Lyα and N V troughs the continuum of 0226−1024 never recovers, relative to the mean non–BALQSO spectrum (note in Fig. 3 how low the O VI broad emission in 0226−1024 lies relative to that in the mean non–

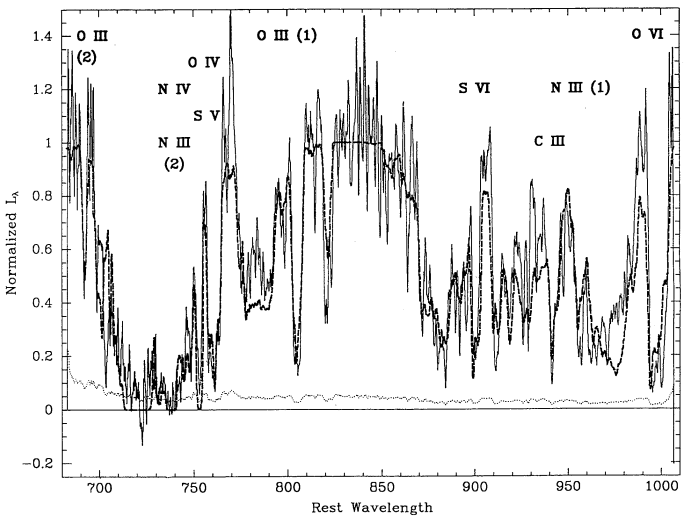

FIG. 5a

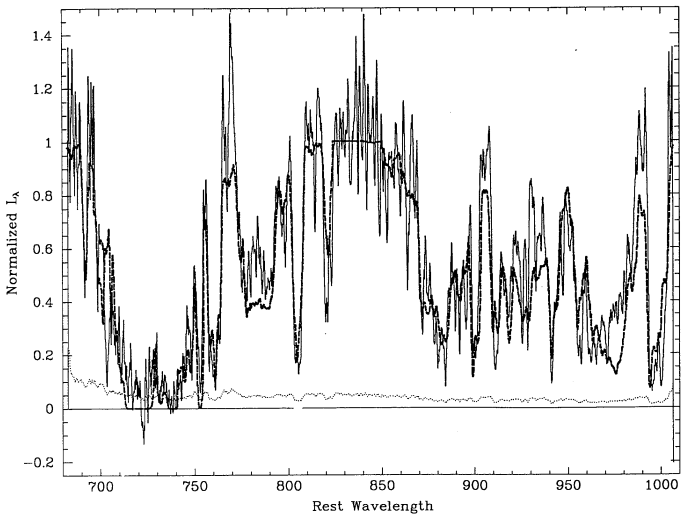

FIG. 5b

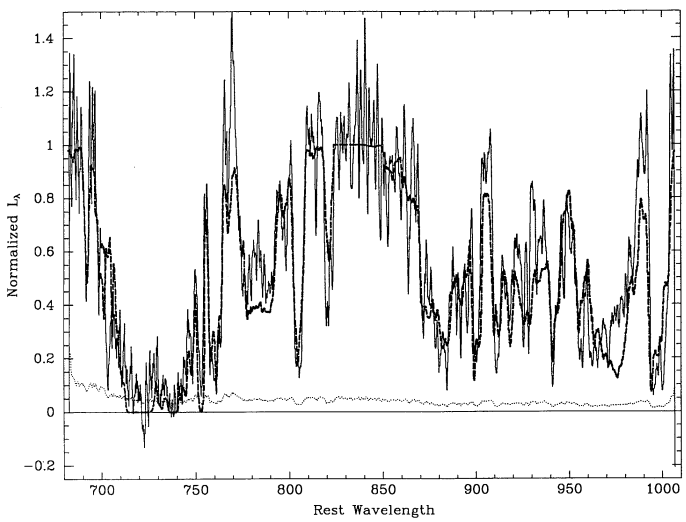

FIG. 5c

FIG. 5.—Comparison between the observed smoothed FOS spectrum (*solid lines*) normalized by the power-law fits, and fitted spectra (*heavy dashed lines*) resulting from the last pass with AMOEBA which chooses the two continuum parameters and the column densities of several ions. AMOEBA minimizes the value of χ^2 characterizing the difference between the observed and fitted spectra. In (*a*) the Ne VIII column density was forced to be zero, in (*b*) the Ne VIII column density was a free parameter, and in (*c*) it was forced to be a constant. In each case the smoothed 1 σ error spectrum is shown (*dots*), normalized by the same power-law fit and divided by the square root of the width (in pixels) of the smoothing boxcar. Those ions whose presence in broad absorption for which we have most confidence are labeled in (*a*) (with accompanying UV multiplet number) with the label being centered roughly over trough (2) of the strongest transition of the absorbing ion (except for the UV2 transition of O III where the label appears over trough [1]).

BALQSO spectrum). Since the emission-line redshift of 0226−1024 is only slightly higher than the mean emission-line redshift of the objects contributing to the non–BALQSO spectrum redward of 1100 Å, and is smaller blueward of 1100 Å, it seems unlikely that differential blanketing due to the Lyα forest is responsible. Note that our mean non–BALQSO spectrum shows no sign of the steep turnover near 1200 Å (see Fig. 3) found for a sample of quasars by Bechtold et al. (1984). So while Pettini & Boksenberg found that the far-ultraviolet continuum of 0946+3009 was consistent with the continua of non–BALQSOs of similar redshift in Bechtold et al., we believe that there could be differences between the continua of non–BALQSOs and the continuum of 0226−1024 (and BALQSOs in general).

It is also possible, however, that these differences could arise from several weak overlapping troughs. Turnshek et al. (1987) found some evidence for broad absorption ascribed to P V and/or Fe III transitions at around 1120 Å (rest) and to S IV at about 1070 Å in 1413+1143. Fe III and S IV meet both criteria given in § 3.1 and were thus considered, although we note that the ionization potential of Fe III (30.65 eV) is smaller than even that of O II. P V does not meet criterion (i) because of its low relative abundance. We also included the possible contribution from a transition arising from a metastable level in C III* (λ1175). Unfortunately, we could not identify any unique absorption features in the data with any of these three ions.

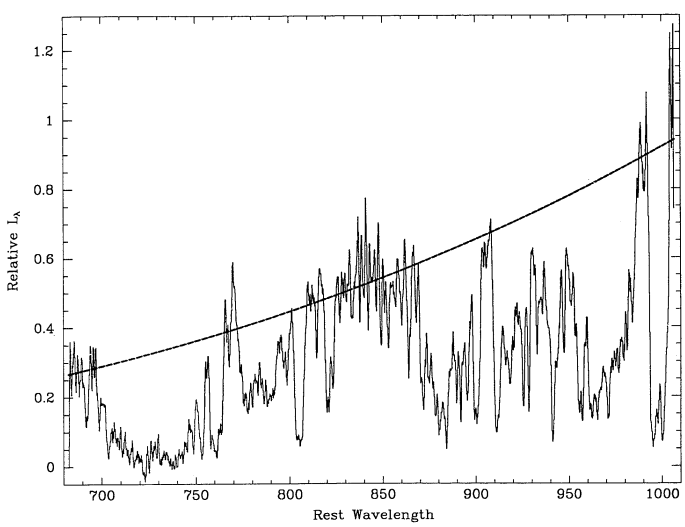

FIG. 6.—The smoothed FOS spectrum is shown with the power-law continuum (*heavy dashed line*) whose parameters were determined by AMOEBA from the run illustrated in Fig. 5*c*. The ordinate has arbitrary units of ergs s^{-1} $Å^{-1}$, after being normalized as in Fig. 3 (see text).

Thus it is not clear to what extent, if any, weak broad absorption is responsible for the depression of the flux in 0226−1024 blueward of Lyα. Therefore, we consider two different assumptions about the effective continuum in the region ∼960–1240 Å. (1) We continue to use the mean non–BALQSO spectrum of sample 1 of Weymann et al. (1991), with the extension down to C III λ977, which we refer to as the "hard" effective continuum. In this case Fe III, S IV, and C III* were included in the fitting. (2) We take the emission lines from the mean non–BALQSO spectrum and place them on the extrapolation of the (lineless) continuum fit to the FOS data (defined by the first two rows of column (7) in Table 2A). We refer to this as the "soft" effective continuum. In this case it is clear that there can be very little absorption from Fe III, S IV, and C III* and so we assume that these ions do not contribute. Figure 7 illustrates these two effective continua in this wavelength range. All of these uncertainties in the effective continuum will of course have some effect on our estimates of the N V and the H I optical depths.

As in our treatment of the FOS data, each component of the N V and Si IV doublets was represented in the fit with a C IV optical depth template, as was Lyα. (The region of the spectrum comprising the C IV trough was of course not included in the fitting procedure, as the template was derived from the C IV.) When fitted, seven transitions of Fe III, two of S IV, and the mean transition from C III* were included. Figure 8*a* shows the fit to the Si IV trough, while Figure 8*b* shows the fit to the region ∼965–1230 Å (including the O VI trough) assuming the "hard" effective continuum, and Figure 8*c* shows the fit to the same region assuming the "soft" effective continuum. In all cases the spectra have first been divided by the effective continuum. Figure 9 shows the estimated individual contributions of Lyα and N V to the optical depth in the N V–Lyα region, assuming the "soft" effective continuum. The substantial narrow absorption in the data near 1185 Å is probably Lyα forest. Comparison of Figures 8*c* and 9 emphasizes that small differences between the fit and data in the residual intensity, near small values of residual intensity, correspond to large differences in optical depth.

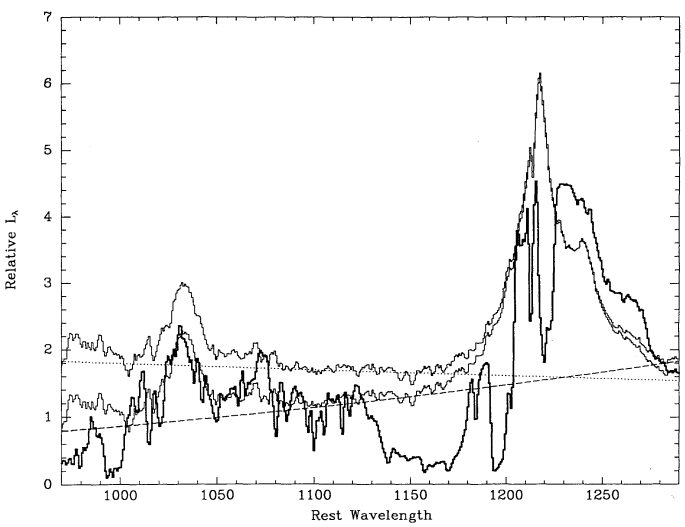

FIG. 7.—The region from 970 to 1290 Å illustrating the two choices for the effective continuum ("hard" and "soft") used for fitting the N V and Lyα troughs over the region from ∼1120 to 1230 Å. The heavy solid line is the adopted observed relative flux of 0226−1024. The top thin solid line is the mean non–BALQSO spectrum which serves as the "hard" effective continuum (as in Fig. 3). The top thin dotted line illustrates a portion of a low-order polynomial fitted to the entire mean non–BALQSO spectrum, which serves as the "hard" (lineless) continuum level. The thin dashed line is the extrapolation of the fitted FOS (lineless) power-law continuum. The emission-line strengths were measured with respect to the mean non–BALQSO spectrum's fitted continuum and added onto the extrapolated fitted FOS power-law lineless continuum. We adopt the resulting spectrum as the "soft" effective continuum (*lower solid thin line*) for the Lyα–N V troughs.

Our determination of the column densities of ions represented in the ground-based data is presented in Table 2B. The values in parentheses were calculated assuming the "soft" continuum, while the others were calculated assuming the continuum has the same shape as the mean non–BALQSO spectrum. The two Fe III column densities given represent the values inferred from the fit depending on whether P V was included in the fit or not (see § 4.4). The Si IV column density was also estimated by integrating over the directly inferred run of Si IV optical depth versus velocity without making use of the C IV template. This estimate was virtually identical to that from the fit using the C IV optical depth template, despite the significant differences between the observed Si IV trough and that predicted by fitting with the C IV template (discussed in § 4.5). We note here that the Si IV broad absorption trough becomes increasingly contaminated blueward of 1290 Å by excess emission in 0226−1024 over the mean non–BALQSO spectrum centered near 1265 Å. According to Baldwin (1992) this emission is likely due to broad Si II λ1263. In addition, we do not place too much significance in the apparent excess absorption in the data over the fit from ∼1360 to 1365 Å in the Si IV trough (see Fig. 8*a*), since this feature does not appear in the 5 m Double Spectrograph data (the remainder of the Si IV absorption profile is very similar in both sets of ground-based data).

As a further check on the reliability of our column density determinations, two of us (M. K., D. A. T.) derived column densities for both the FOS and ground-based data completely independently. A double power law with a break near N V λ1240 was used to fit the continuum to the combined MMT optical and FOS spectrum. Grillmair & Turnshek (1987) describe the method used. These results are presented in column (8) of Table 2A and column (3) of Table 2B under the heading of "KT." The similarities of the results from the two independent analyses show that our column density estimates are reliable, within the assumptions and limitations described above, and the differences between the column densities of columns (2)–(7) and (8) reflect fairly well the uncertainties derived from the AMOEBA fitting alone.

4. DISCUSSION OF THE RESULTS

4.1. *General Comparisons between Data and Fit*

Looking at Figures 5*a*, *b*, *c* one can see that the fit is very successful. It can account for most of the major features in the FOS data. We consider this remarkable, considering the uncertainties and our simplifying assumptions. However, there are a number of regions where the fit does not match the data within the errors. Most notable of these is the 970–1000 Å, including trough (3) of O VI. This discrepancy may in part be due to the method of determining the effective continuum. In addition to the uncertainty in the intrinsic continuum level, broad emission due to C III λ977 and possibly N III λ990 will act to raise the effective continuum in this region. Figures 8*a*, *b*, *c* also show generally good fits to the ground-based data, given the assumptions we make about the effective continuum. We

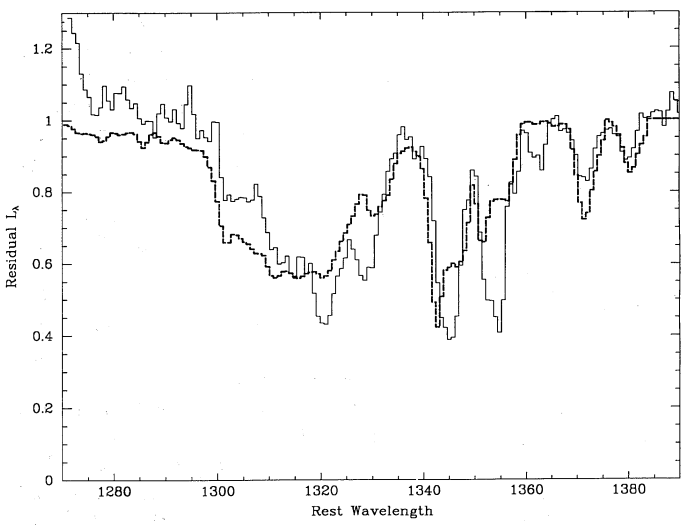

FIG. 8*a*

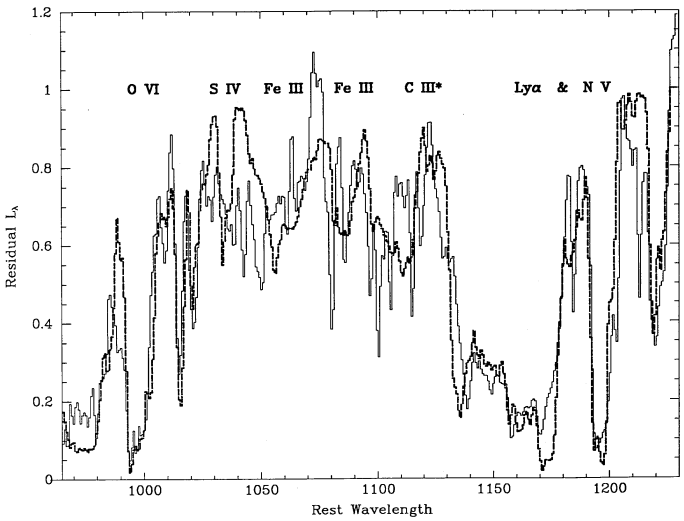

FIG. 8*b*

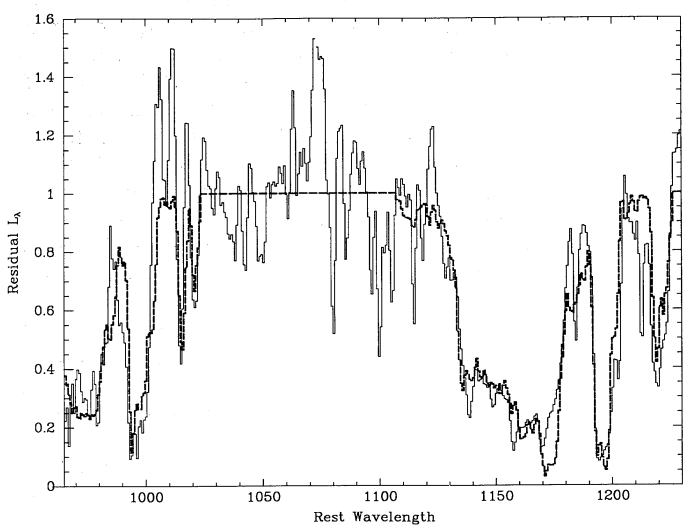

FIG. 8*c*

FIG. 8.—Comparison between the observed (*thin solid line*) and fitted spectra (*heavy dashed line*) for the ground-based data. Si IV is shown in (*a*), assuming the mean non–BALQSO spectrum is the effective continuum. Note in (*a*) that the doublet ratios in trough (1) (~1370–1382 Å) and especially in trough (2) (~1342–1355 Å) are nearly unity, as expected for an optically thick transition, even though the line centers are very far from black. N V–Lyα, O VI, S IV, Fe III, and C III* are shown in (*b*), assuming the "hard" effective continuum. The BAL ions are labeled in (*b*) roughly over the position of trough (2) for that ion, the exception being C III* whose label appears between troughs (2) and (3). N V–Lyα and O VI are shown in (*c*), assuming the "soft" effective continuum (which effectively excludes any significant absorption from S IV, Fe III, or C III*).

discuss in more detail below the comparisons between the data and the fit.

4.2. *The Presence of* Ne VIII

If Ne VIII is actually present to anything like the degree suggested by either of the two fits in which it was not forced to be zero, this would indicate that a significant amount of BAL region gas was very highly ionized [I.P. (create Ne VIII) = 207.27 eV]. Unfortunately, as one can see from Figures 5*a*, *b*, *c*, there is little difference in how well the data are fitted, whether or not one includes Ne VIII. This is true except for the double-peaked structure near 770 Å. It happens that trough (1) of the weaker transition of the Ne VIII doublet falls directly into the observed trough near 768 Å (see Fig. 10). The fact that our fitted continuum falls somewhat below the observed peak flux may be due partly to broad-line emission from N III and N IV in this vicinity; the effect of this was to drive down the predicted column density of Ne VIII when it was taken to be a free parameter. If this double-peaked structure is due to broad absorption, it may very well be the signature of Ne VIII. No other ion has a trough that can account for it. Tests show that if the double-peaked structure near 770 Å is, in fact, due entirely to Ne VIII absorption, then a Ne VIII column of at least $\sim 4 \times 10^{16}$ cm^{-2} must be present. However, given the assumption of relative solar abundances and our determination of the C IV column density, even if all of the neon in the BAL gas were in ionization stage VIII, the column density would fall short of the value above by a factor of ~2.5, unless a large fraction of the C was in the form of C V. (We note here that similar difficulties

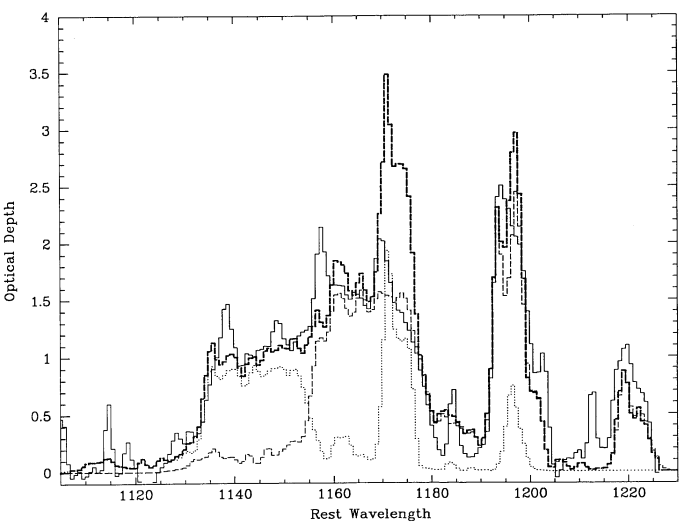

FIG. 9.—The contribution of N V (*thin dashed line*) and Lyα (*dots*) to the total fitted optical depth (*thick dashed line*). The thin solid line represents the optical depth inferred from the observed flux and the "soft" effective continuum.

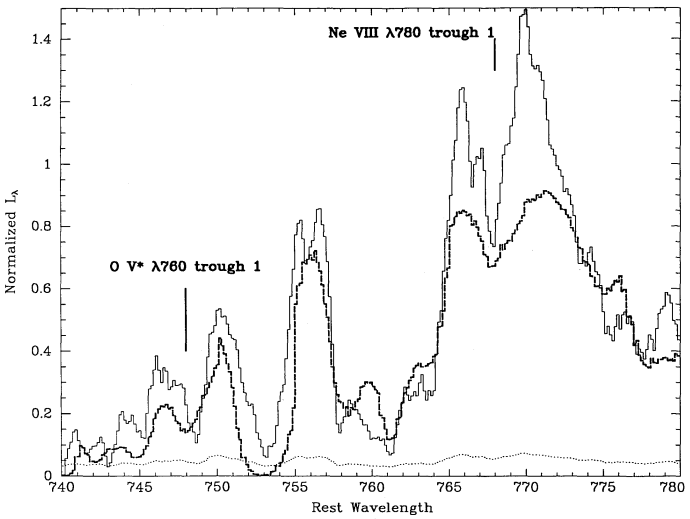

FIG. 10.—An expansion of Fig. 5*c* in the region where possible unique absorption features belonging to trough (1) of O V* λ760, at 748 Å, and to trough (1) of Ne VIII λ780, at 768 Å, as marked, might be attributed.

occur with the predicted column densities of the Si IV and the sulfur ions.) However, a few fortuitously placed Lyα forest lines might also account for the feature. Unfortunately, there is no other feature in the present data that may be unambiguously associated with Ne VIII (the fits between 720 Å and 750 Å differ slightly, but this region mainly lies near or within the noise; see Figs. 5*a*, *b*, *c*). In summary, while there is evidence for broad absorption due to Ne VIII, it is not entirely convincing. Observations of other BALQSOs, with relatively simple yet distinctive trough signatures, will be needed to resolve this issue.

4.3. *The Presence of Excited State Metastable* O V*, N IV*, *and* C III*

Pettini & Boksenberg (1986) found evidence for broad absorption by O V* λ760.36, a transition from a metastable level lying 10.2 eV above the ground state, from *IUE* observations of the BALQSO 0946+3009. The fits to the 0226−1024 observations also suggest a substantial column density in this ion (see Table 2A). In particular, there are two spectral features in the data which suggest its presence (see Figs. 5 and 10). First, excluding O V* from the list of absorption features results in fits which severely underpredict the absorption from 700 to 720 Å. Second, trough (1) of O V* falls into the absorption features centered near 748 Å. No other ion can account for this feature, if it can be attributed to broad absorption. Could there be any other ion which might be contributing to the absorption from 700 to 720 Å ascribed to O V*? Ar VI λ757 is one possibility, but as discussed earlier we believe a substantial presence of this ion to be unlikely. N IV λ765, which is not well constrained by the fits, could account for the absorption down to 700 Å only if its column density exceeded 10^{17} cm^{-2}, but this does not seem likely, given the derived N III and N V column densities. N III λ764 cannot help much since its trough strength is constrained by that of N III λ991, which is itself fairly well constrained by the data. In general, the troughs of both of these ions lie too far to the red to contribute effectively. The only other transitions known to lie in this region are Ne I λ744 (UV 1) and Ne I λ736 (UV 2). The first of these lies near the optimal spot to provide extra absorption, but it has a very small oscillator strength, while the latter lies too far blueward for its trough (3) to provide the required absorption. Moreover, we expect little Ne I for the reasons explained in § 3.1.

We found an upper limit to the column density of metastable N IV* λ923 of $\sim 10^{15}$ cm^{-2}, which is negligible. A slightly larger column density for C III* λ1175 of $\sim 5 \times 10^{15}$ cm^{-2} is inferred from the fit if the depression in the continuum in 0226−1024 relative to the mean non–BALQSO spectrum between 1000 and 1200 Å can be attributed to broad absorption (trough [3] of C III* is the depression in the fitted spectrum located redward of roughly 1095 Å in Fig. 8*b*).

Despite the observational evidence just discussed for the presence of absorption arising from metastable levels in C III* and O V* in 0226−1024, and from O V* in 0946+3009 by Pettini & Boksenberg (1986), there are some rather strong arguments against the reality of this absorption, especially for the case of O V*.

First, while the column densities inferred for the metastable O V* and C III* terms are fairly comparable with their ground-term counterparts, this is not the case for the metastable N IV* column density, and this is rather difficult to understand.

Second, a column density in O V* comparable to that of the ground term would require not merely a high-density gas, as noted by Pettini & Boksenberg, but would also require that the gas be very hot as well in order to populate the metastable levels by collisions from the ground state. A rough estimate based upon a simple two level atom (assuming the J levels of the $^3P^o$ term are in statistical equilibrium) and utilizing the collisional rates of Dufton et al. (1978) and the transition probabilities of Nussbaumer & Storey (1979) indicates that at a temperature of 1×10^5 K an electron density $\sim 3 \times 10^{11}$ cm^{-3} is required to produce a population in the $^3P^o$ term comparable to that in the ground state. At a temperature of 7.5×10^4 K the required density rises to $\sim 5 \times 10^{11}$ cm^{-3}.

In principle, an intense radiation field could also populate the $^3P^o$ term via a cycle of photoionizations from the O V ground state followed by recombinations from O VI to the O V $^3P^o$ term, without the necessity of an extremely hot gas. This would require a photoionization rate of order $A(^3P^o–^1S)_{\rm eff} \sim 700$ s^{-1}. However, the fact that the O VI column density does not appear to greatly exceed our derived O V* column density and appears to be in fact comparable to the O IV column density (see Tables 2A, 2B) suggests that the O V ground-state column density (whose transitions lie shortward of our FOS spectrum) should be comparable to the O VI column density. This limits the O V–O VI photoionization rate to some value which is proportional to the assumed electron density. At electron densities high enough for collisions to begin to populate the $^3P^o$ term (e.g., $\sim 5 \times 10^{11}$ cm^{-3}) we estimate the photoionization rate to fail by about two orders of magnitude to significantly populate the $^3P^o$ term. At even higher densities, collisional de-excitation from the $^3P^o$ term dominates over radiative de-excitation, depopulating the $^3P^o$ term at a rate proportional to the electron density. Therefore, our conclusion is that a very hot, very dense gas would be required to significantly populate the $^3P^o$ term.

Nevertheless, the photoionization rate required by ionization equilibrium between O V and O VI at densities of $\sim 5 \times 10^{11}$ cm^{-3} is very much higher than what one expects assuming a typical shape to the far-UV radiation field (e.g., Mathews & Ferland 1987) unless the BAL region is much closer by a factor of ~10–30 to the presumed compact source of high-energy photons than the ~1–3 pc often assumed. Thus, if the presence of absorption from the $^3P^o$ term of O V *were* to

be confirmed, it would suggest not only the presence of a very hot, very high density gas, but a very hard radiation field and/or a very small size for the BAL region. This in turn would require an even smaller region for the broad emission-line region, since N v absorption strongly absorbs the Lyα emission (see Fig. 7). While such sizes and densities may seem extreme, Baldwin et al. (1992) have recently shown that comparably high densities are likely to be present in the broad *emission*-line regions of some QSOs and when they are, they produce abnormally strong Fe III and Al III emission, a property characteristic of BALQSOs. A significant range of densities is likely to be required to produce the range of ionization which may be present in the BAL clouds.

However, even granting such high electron densities, it is very difficult to understand how to produce the required very high electron temperatures. In principle, heating by free-free absorption from far-infrared radiation ($\lambda > 50$ μm) can heat the gas to high temperatures, but such radiation is now thought to arise from dust and thus to be quite extended, so that the energy density is not high. Particle heating or mechanical dissipation would seem to be required in an amount exceeding by at least an order of magnitude the energy input from the radiation field.

Even if such large additional energy input were present, a significant fraction of this energy would be radiated away via collisionally excited line emission due to C IV, N V, and especially O VI. In order for this emission not to significantly exceed the total observed line emission, the global continuum source covering factor of such a hot, high-density gas would have to be 5% or less. This is significantly smaller than the value of $\sim 10\%$ generally taken to be the global source covering factor of the BAL gas.

Evidently, confirming or disproving the possible presence of metastable O V, N IV, and C III absorption in other BALQSOs is an important problem. As is the case with Ne VIII, further observations of other BALQSOs will be needed to confirm or disprove their presence. FOS–*HST* spectra of 0946+3009 recently obtained by two of us (V. J. and E. M. B.) and other members of the FOS team will provide important new data in this connection.

4.4. *The Presence of* Fe III, S IV, *and* P IV, V

Whether significant broad line absorption between the Lyα and O VI troughs is actually present depends where one decides the true effective continuum level in 0226−1024 lies. Looking at Figure 8*b* one could conclude that the data are not inconsistent with the possibility that the depression in the continuum relative to the mean non–BALQSO spectrum between 1000 and 1200 Å (see Fig. 7) can be attributed to broad absorption. The "emission-like" feature near 1075 Å in the spectrum of 0226−1024 is real, since it appears in both sets of ground-based data. We find it highly unlikely, however, that it is due to a broad emission line. The only transition near here is S IV λ1070, a weak transition. This feature may be indicative of weak broad line absorption on either side of it, rather than a continuum reddening-type absorption or other type of very broad band depression. There are 18 transitions from the three ions Fe III, S IV, and P V between ~ 1000 and 1130 Å, which, even if individually weak, can sum up to substantial absorption in this region, as shown in Figure 8*b*. A significant presence of S IV would not surprise us. However, the large inferred column in Fe III (2×10^{16} cm^{-2}; Table 2B) would be surprising considering its relatively low ionization potential. To address the possibility of a significant overabundance in phosphorus, we also attempted fits to the data which included the relevant transitions of P V (see Table 1). When we included P V $\lambda\lambda$1118, 1128 in the fitting of the ground-based data, we found an upper limit to its column density of roughly 2×10^{15} cm^{-2}. Interestingly, its inclusion caused the Fe III column density to fall to a slightly more plausible 5×10^{15} cm^{-2}. The fit is as good as or slightly better than the one in Figure 8*b*. Even a column density of 2×10^{15} cm^{-2} in P V, however, would imply an overabundance of phosphorus relative to carbon of order 10^2. Since the ionization of P IV and P V are so very similar to that of C III and C IV, the P IV:P V column density ratio ought to be roughly that of C III:C IV (1:5). This ratio for P IV:P V along with the column density of P V given above imply an optical depth in P IV λ951 of $\sim 6\%$ that of C IV. An optical depth that small lying among the strong troughs of C III, N III, and S VI cannot be excluded. Thus we cannot exclude the possibility of a significant overabundance in phosphorus. Higher resolution and higher S/N ratio data covering the spectral region 1000–1200 Å will be needed to better determine the presence of these ions.

4.5. *Discrepancies Involving the* C IV *Template*

Inspection of Figures 5 and 8 reveals that there are some significant discrepancies between the observed and fitted spectra which cannot be reconciled with any single optical depth scaling factor. This could arise from one of two main sources. (1) The assumption that the ionization is independent of velocity is false. (2) One of our other assumptions (e.g., that the clouds cover the effective continuum source) is false. We discuss each of these possibilities in turn.

4.5.1. *Is Ionization a Function of Velocity?*

There has been some discussion in the literature as to whether there are significant differences in the ionization of the BAL gas as a function of velocity, and if so, whether there are systematic trends in such differences. By comparing the optical depth profiles of C IV and Si IV, Junkkarinen et al. (1987) found evidence in PHL 5200 and possibly three other BALQSOs for a systematic increase in ionization at large outflow velocities. They discussed possible changes in ionization from trough to trough and within individual troughs. The analysis here is made especially difficult due to the uncertainties associated with the assumption of an effective continuum in the vicinity of the weak Si IV trough.

Examination of this question is only feasible in 0226−1024 for those ions whose troughs do not overlap with troughs of other ions: O III λ835, O VI λ1034, and Si IV λ1397. By comparing the fit to the data, based upon the C IV template, to the observed troughs we can infer possible diferences in ionization as a function of velocity. Unfortunately, to some extent in each case, unaccounted broad emission from the same transition observed in broad absorption, other unaccounted broad emission transitions, and the uncertainty of the intrinsic continuum level confuse the analysis. Of these, Si IV suffers the least from these problems, being affected primarily shortward of 1290 Å as mentioned above. Figure 8*a* shows significant differences between the fit and the data, and we discuss these in more detail in the next section.

The other believable discrepancy involving the C IV template lies in the broad trough of the N V–Lyα absorption, between ~ 1170 and 1180 Å (Fig. 8*c*). There appears to be a small but significant difference between the data and fit in this region.

Although the Lyα and N v troughs do overlap, they do so in such a way that the narrow trough (2) of Lyα overlaps only the red half of the broad trough (3) of N v, making them distinguishable here. Examination of the region 1130–1170 Å in Figure 9 reveals that the broad trough is well fitted by the sum of troughs (3) of N v and Lyα. The entire discrepancy between ~1170 and 1180 Å arises because of trough (2) of Lyα. We could remove this discrepancy if the ratio of the Lyα to C IV optical depths in trough (2) is at least 5 times smaller than the optical depth ratio in trough (3). This is true for either of the effective continua assumed in this region. If one assumes this difference to be due to a difference in ionization between troughs (2) and (3), then trough (2) must be highly ionized with very little column density in H I.

4.5.2. *Do the BAL Clouds Cover the Continuum Source?*

The question of whether the ensemble of BAL clouds cover the (effective) continuum source has been discussed by Kwan (1990). This issue has an important bearing on whether the photoionization models can successfully model the observations as well as on the question of whether there are strong abundance anomalies in the BAL region (cf. Kwan 1990). The present data provide some direct evidence on this point independent of our fitting proceedure. Referring to Figure 8*a* we can see that the doublet transitions in Si IV in both troughs (1) and (2) are well separated. Note especially in trough (2) (~1340–1360 Å) that the doublet ratio is nearly 1. This is evidence that the BAL clouds are optically thick in this trough for these transitions. However, since the troughs are far from black, the absorbers may not cover the entire continuum source. This was one of our primary assumptions in the determination of the optical depth from the residual intensity. Under this interpretation, the extent to which the absorbing clouds do not completely cover the continuum source is apparently ion-dependent (compare the residual intensity of Si IV to O VI) and may also be velocity-dependent as well. This situation may extend to trough (3) and for many or most of the ions observed in absorption. Coverage of the effective continuum which varies with outflow velocity and from ion to ion can mimic changes in ionization as a function of outflow velocity. Moreover, there is likely to be some coupling between the covering factor and the actual level of ionization. For example, if the clouds had dense small cores and lower density envelopes, the high-density cores with small covering factors would tend to have lower levels of ionization than the larger, lower density envelopes. Such a model has recently been proposed by Williams (1992) to account for the emission spectrum of novae shells. This scenario is consistent with the trends in the depths of the Si IV, C IV, and O VI troughs. However, there is a problem with the depth of the O III absorption in trough (2) near 805 Å, with a residual intensity of roughly 15% (see Fig. 5). O III has an ionization potential closer to that of Si IV than to C IV, and yets its covering factor must be quite high in the partial covering scenario. This problem probably extends to the depth of the C III λ977 absorption in trough (2) near 940 Å as well. Of course, rather than a simple comparison of ionization potentials, we really need to know in detail how the ions within a given element are distributed, given a level of ionization and the shape of the ionizing continuum. This will be investigated in future work.

4.5.3. *Are There Unresolved Narrow Lines in the BAL Troughs?*

An alternative possibility to the incomplete coverage hypothesis is that these features (e.g., the doublet components to trough (2) in Si IV) are composed of nearly black, intrinsically very sharp features well below our spectral resolution. The Si IV doublet ratio in trough (2) shown in Figure 8*a* indicates an optical depth at line center of ~10–100. Simulations show that about 80 optically thick clouds having thermal widths corresponding to a temperature of 20,000 K and spread over about 1000 km s^{-1} could account for the observed depths of trough (2) of Si IV and C IV in our low-resolution data. This model requires that there be very little macroscopic motion present, since velocities only 20% of the hydrogen thermal width would mask the difference between the C IV and Si IV thermal widths. It also implies that, with all else equal, the less massive the ion, the deeper should be the trough. However, the fact that the doublet splitting for Si IV (~2000 km s^{-1}) is large compared to the width of trough (2) while that for C IV (~500 km s^{-1}) is small is also an important contributing factor. The same simulations also show that the "picket fence" structure expected in this model should be readily observable at high resolution even at modest S/N. We intend to check this alternative possibility by obtaining high-resolution data in the Si IV region.

5. SUMMARY

We have identified up to 18 ions in broad absorption in the wavelength range 680–1550 λ in the BALQSO 0226−1024. While some of these ions can, in principle, be studied from the ground from high-redshift BALQSOs, the much denser Lyα forest and the frequent occurrence of Lyman limit systems makes this very difficult. Column densities have been estimated for all of these. Significant absorption by O V from a metastable state and Ne VIII may be present, but the evidence for either is not conclusive. Both are of interest, since the former implies very high values for the electron density and temperature in the BAL gas (and, if photoionization still dominates over collisional ionization under such conditions, a very high value for the intensity of the radiation field), while the latter implies the existence of very highly ionized gas. We have also presented evidence that the BAL clouds are optically thick and either do not completely cover the continuum source, or consist of large numbers of sharp unresolved lines.

Whereas previous photoionization calculations for the BAL clouds were constrained by only a handful of ionic column densities, calculations may now utilize a dozen or so. In particular, because we have estimated column densities for two to three ions of carbon, nitrogen, oxygen, and sulfur, the abundances of these ions will be much better constrained in the photoionization models than was previously the case. Conversely, it will be difficult to appeal to abundance discrepancies to explain ionization anomalies, and an appeal to incomplete coverage of the continuum source which is ion and outflow velocity-dependent may have to be made. These issues will be discussed in a future paper.

We thank Dr. Robert Williams for comments on the manuscript, and Dr. Gordon MacAlpine, the discoverer of 0226−1024, for generously making available his unpublished *IUE* spectrum of 0226−1024. Although too noisy to identify the troughs, it indicated that there was measurable flux and thereby encouraged us to select this object to observe with FOS. C. B. F. acknowledges support through NSF grant AST 90-01181. R. J. W., S. L. M., and K. T. K., acknowledge support through NASA grant NAG-5-1859 and NSF grant AST 90-05117.

REFERENCES

Baldwin, J. A. 1992, private communication
Baldwin, J. A., Carswell, R. F., Ferland, G. J., Phillips, M. M., Wilkes, B. J., & Williams, R. E. 1992, in preparation
Barlow, T. A., Junkkarinen, V. T., & Burbidge, E. M. 1989, ApJ, 347, 674
Barlow, T. A., Junkkarinen, V. T., Burbidge, E. M., Weymann, R. J., Morris, S. L., & Korista, K. T. 1992, ApJ, 397, 81
Bechtold, J., Green, R. F., Weymann, R. J., Schmidt, M., Estabrook, F. B., Sherman, R. D., Wahlquist, H. D., & Heckman, T. M. 1984, ApJ, 281, 76
Begelman, M. C., de Kool, M., & Sikora, M. 1991, ApJ, 382, 416
Braun, E., & Milgrom, M. 1990, ApJ, 349, L35
Chaffee, F. H., Foltz, C. B., Hewett, P. C., Francis, P. J., Weymann, R. J., Morris, S. L., Anderson, S. F., & MacAlpine, G. M. 1991, AJ, 102, 461
Drew, J. E., & Boksenberg, A. 1984, MNRAS, 211, 813
Dufton, P. L., Berrington, K. A., Burke, P. G., & Kingston, A. E. 1978, A&A, 62, 111
Foltz, C. B., Chaffee, F. H., Hewett, P. C., MacAlpine, G. M., Turnshek, D. A., Weymann, R. J., & Anderson, S. F. 1987, AJ, 94, 1423
Foltz, C. B., Chaffee, F. H., Hewett, P. C., Weymann, R. J., Anderson, S. F., & MacAlpine, G. M. 1989, AJ, 98, 1959
Grevesse, N., & Anders, E. 1989, Cosmic Abundances of Matter, AIP Conf. Proc. ed. C. J. Waddington (New York: AIP), 183
Grillmair, C. J., & Turnshek, D. A. 1987, poster paper, QSO Absorption Lines: Probing the Universe, ed. J. C. Blades, C. Norman, & D. A. Turnshek, 1
Hamann, F., Korista, K., & Morris, S. 1992, ApJ, submitted
Hartig, G. F., & Baldwin, J. A. 1986, ApJ, 302, 64
Hewett, P. C., Foltz, C. B., Chaffee, F. H., Francis, P. J., Weymann, R. J., Morris, S. L., Anderson, S. F., & MacAlpine, G. M. 1991, AJ, 101, 1121
Junkkarinen, V. T. 1983, ApJ, 265, 73
Junkkarinen, V. T., Burbidge, E. M., & Smith, H. E. 1983, ApJ, 265, 51
———. 1987, ApJ, 317, 460
Kwan, J. 1990, ApJ, 353, 123
Mathews, W. G., & Ferland, G. J. 1987, ApJ, 323, 456
Morris, S. L. 1988, ApJL, 330, L83
Morris, S. L., Weymann, R. J., Anderson, S. F., Hewett, P. C., Foltz, C. B., Chaffee, F. H., Francis, P. J., & MacAlpine, G. M. 1991, AJ, 102, 1627
Morton, D. C. 1991, ApJS, 77, 119
———. 1992, private communication
Nussbaumer, H., & Storey, P. J. 1979, A&A, 74, 244
Pettini, M., & Boksenberg, A. 1986, New Insights in Astrophysics: 8 Years of UV Astronomy with IUE, ed. E. J. Rolfe (ESA Pub.), 627
Press, W. H., Flannery, B. P., Teukolsky, S. A., & Vetterling, W. T. 1986, Numerical Recipes: The Art of Scientific Computing (Cambridge: Cambridge University Press)
Smith, L. J., & Penston, M. V. 1988, MNRAS, 235, 551
Sprayberry, D., & Foltz, C. B. 1992, ApJ, 390, 39
Stocke, J. T., Morris, S. L., Weymann, R. J., & Foltz, C. B. 1992, ApJ, submitted
Surdej, J., & Hutsemekers, D. 1987, A&A, 177, 42
Turnshek, D. A. 1984a, ApJ, 280, 51
———. 1984b, ApJL, 278, L87
———. 1988, QSO Absorption Lines: Probing the Universe, ed. J. C. Blades, D. A. Turnshek, & C. A. Norman (Cambridge: Cambridge University Press), 17
Turnshek, D. A., Briggs, F. H., Foltz, C. B., Grillmair, C. J., & Weymann, R. J. 1987, poster paper: QSO Absorption Lines: Probing the Universe, ed. J. C. Blades, C. Norman, & D. A. Turnshek, 8
Turnshek, D. A., Weymann, R. J., Carswell, R. F., & Smith, M. G. 1984, ApJ, 277, 51
Weymann, R. J., Morris, S. L., Foltz, C. B., & Hewett, P. C. 1991, ApJ, 373, 23
Weymann, R. J., Turnshek, D. A., & Christiansen, W. A. 1985, Astrophysics of Active Galaxies and Quasi-Stellar Objects, ed. J. S. Miller (Mill Valley: University Science Books), 333
Wiese, W. L., Smith, M. W., & Glennon, B. M. 1966, Atomic Transition Probabilities, Vol. 1, Hydrogen through Neon (Washington: NBS)
Wiese, W. L., Smith, M. W., & Miles, B. M. 1969, Atomic Transition Probabilities, Vol. 2, Sodium through Calcium (Washington: NBS)
Williams, R. E. 1992, preprint